

acceptor orbital, as perturbed by the central ion, etc. This is true whether electron transfer takes place by a conjugatively stabilized radical-cation transition state as suggested by Gould^{4c} or by a resonance mechanism following preparation of the acceptor and donor sites as suggested by Price and Taube.^{4b} If, then, for a given reducing agent, this orbital were the main factor in determining the energy barrier, it would have been reasonable to expect the transfer of one electron to Co^{III} to be at least as fast as the transfer of the two electrons to the "free" ligand. The fact then that this is not the case indicates that the rate is determined by other factors, e.g., preparation of the acceptor and donor sites as suggested by Price and Taube.

In continuing the comparison it is also interesting to note that the product Cr₂l_c⁴⁺ obtained in the reaction of Cr²⁺ (aqueous) with "free" pyruvic acid has ϵ_{\max} 59 at λ_{\max} 420 nm and ϵ_{\max} 45 at λ_{\max} 570 nm. These absorptivity values indicate that one of the two Cr^{III} ions forms with the ligand a chelated ring. In contrast, the product, and presumably the activated complex as well, in the reduction of the pyruvato complex of Co^{III} is monodentate. In fact it has been suggested^{4b,c} in this case that chelation in the activated complex is not an important factor in determining the relative rates. Extension of this conclusion to include the reduction of the "free" ligand as well cannot be made offhand. The differences in rates between the bound and the unbound ligand are clearly associated with structural differences.

Acknowledgments. The authors thank Mrs. K. Kaplany-Aravany for secretarial assistance and Mrs. E. Kissa-Meidany for laboratory assistance. We also thank the Analytical Laboratory of N.R.C. "Demokritos" for analytical work.

References and Notes

- (1) University of Athens, Laboratory of Inorganic Chemistry, Navarinou 13a, Athens.
- (2) (a) A. Malliaris, and D. Katakis, *J. Am. Chem. Soc.*, **87**, 3077 (1965); (b) E. Vrachnou-Astra and D. Katakis, *ibid.*, **89**, 6772 (1967); (c) E. Vrachnou-Astra, P. Sakellaridis, and D. Katakis, *ibid.*, **92**, 811 (1970); (d) *ibid.*, **92**, 3696 (1970); (e) E. Vrachnou-Astra and D. Katakis, *ibid.*, **95**, 3814 (1973); (f) D. Katakis and E. Vrachnou-Astra, *Chim. Chronika, New Ser.*, **1**, 210 (1972); (g) *ibid.*, **1**, 225 (1972); (h) E. Vrachnou-Astra and D. Katakis, *J. Am. Chem. Soc.*, **97**, 5357 (1975).
- (3) J. B. Conant and H. B. Cutter, *J. Am. Chem. Soc.*, **48**, 1016 (1926).
- (4) (a) H. J. Price and H. Taube, *J. Am. Chem. Soc.*, **89**, 269 (1967); (b) H. J. Price and H. Taube, *Inorg. Chem.*, **7**, 1 (1968); (c) E. S. Gould, *J. Am. Chem. Soc.*, **96**, 2373 (1974).
- (5) The term "free ligand" is used here in the sense that it is not complexed beforehand. After mixing with the reductant, however, complexation is a necessary step for further reaction.
- (6) (a) F. A. Loewus, P. Ofner, H. F. Fisher, F. H. Westheimer, and B. Venesland, *J. Biol. Chem.*, **202**, 699 (1953); (b) R. H. Abeles, R. F. Hutton, and F. H. Westheimer, *J. Am. Chem. Soc.*, **79**, 712 (1957).
- (7) E. L. King, and E. B. Dismukes, *J. Am. Chem. Soc.*, **74**, 1674 (1952).
- (8) D. E. Tallman, and D. L. Leussing, *J. Am. Chem. Soc.*, **91**, 6253, 6256 (1969).
- (9) A. Yoe and A. L. Jones, *Ind. Eng. Chem., Anal. Ed.*, **16**, 11 (1944).
- (10) M. Becker, *Z. Electrochem.*, **68**, 669 (1964).
- (11) H. Strehlow, *Z. Electrochem.*, **66**, 392 (1962).
- (12) P. George, and J. S. Griffith, "The Enzymes", Vol. 1, Academic Press, New York, N.Y. 1959, Chapter 8.

Electron Spin Resonance Line-Width Alternation and Na⁺ Transfer in the Ion Pairs of 3,5-Dinitropyridine

M. Barzagli, P. Cremaschi, A. Gamba,¹ G. Morosi, C. Oliva, and M. Simonetta*

Contribution from the C.N.R. Center for the Study of Structure/Reactivity Relations and Institute of Physical Chemistry, University of Milan, 20133 Milan, Italy.

Received August 17, 1977

Abstract: An ESR study of the ion pairs of 3,5-dinitropyridine with alkali metals in tetrahydrofuran and 1,2-dimethoxyethane is reported. The analysis of the ESR spectra of the ion pair with Na⁺ after the addition of sodium tetraphenylborate shows an intermolecular cation transfer between DNP⁻·Na⁺ and Na⁺BPh₄⁻. Kinetic parameters are compared with those of the corresponding reaction of *m*-dinitrobenzene. The interpretation of the ion pairs structure is supported with ab initio calculations of the electrostatic potential generated by the 3,5-dinitropyridine radical anion. The spin distribution in the ion pair is computed by the McLachlan method modified according to McClelland. The same method is adopted to study the exchange mechanism by evaluating the association energy for the triple ions.

Introduction

Line-width alternation effects in the ESR spectra of a number of ion pairs obtained by alkali metal reduction of aromatic substrates have been widely investigated.² These effects are generated by the relative motions of the counterions causing various magnetic field modulations; thus the line width is essentially a kinetic parameter, and allows a description of the ion pair dynamics.

Following a research on radical ions of nitropyridine derivatives,³⁻⁵ we have previously determined the hfs constants of the free radical anion of 3,5-dinitropyridine (DNP) obtained by electrolytic reduction in different solvents.^{6,7}

In this paper we report an ESR study of ion pair association of DNP with alkali metals in tetrahydrofuran (THF) and

1,2-dimethoxyethane (DME). Information on the structure of the ion pairs is also obtained by the electrostatic potential method based on an ab initio wave function.⁸⁻¹⁰

In particular we investigate the rate and the mechanism of sodium exchange reaction in the DNP⁻·Na⁺ system when another source of metal ions, such as sodium tetraphenylborate (NaBPh₄), is added to the solution.

A comparative analysis of the ESR spectra of *m*-dinitrobenzene (MDNB)-sodium after the addition of NaBPh₄¹¹ is presented.

Experimental Section

DNP was obtained following the method suggested by Plazek,¹² mp 106 °C. NaBPh₄ (Fluka) was used without additional purification.

Table I. Experimental hfs Constants (G) of $\text{DNP}^-\cdot\text{M}^+$ in DME and THF

Solvent	Redn method	$t, ^\circ\text{C}$	$a_{\text{N}(-\text{N}=\text{O})}$	$a_{\text{H}_2}; a_{\text{H}_6}$	a_{H_4}	$a_{\text{N}(3-\text{NO}_2)}; a_{\text{N}(5-\text{NO}_2)}$	a_{M}
DME	Li	20	1.38	3.46; 4.19	3.54	9.37; 0.30	0.26
	Na	20	1.37	3.52; 5.16	3.68	8.73; 0.27	0.27
	Na + NaBPh ₄ (0.4 M)	20	1.38	4.51 ^a	3.62	4.41 ^b	0.00
		-60	1.40	3.48; 5.26	3.76	8.53; 0.00	0.00
THF	K	20	1.34	3.45; 5.10	3.45	7.87; 0.25	0.00
	Li	20	1.36	3.60; 5.00	3.60	9.13; 0.25	0.00
	Na	20	1.37	3.53; 5.11	3.63	8.82; 0.27	0.25
	Na + NaBPh ₄ (0.04 M)	20	1.38	4.35 ^a	3.62	4.43 ^b	0.00
		-60	1.41	3.00; 5.10	3.55	8.28; 0.00	0.00
	K	20	1.38	3.57; 5.28	3.57	8.17; 0.00	0.00
THF	Cs	20	1.38	3.65; 5.34	3.65	8.14; 0.00	2.19
	Electrolysis	20	1.45	4.85; 4.85	3.36	3.52; 3.52	

^a In the fast exchange region only the averaged value of a_{H_2} is detectable. ^b As the components of the hyperfine quintet with $M_{\text{N}} = \pm 1$ are very broadened, only a triplet with splitting $a_{\text{N}(3-\text{NO}_2)} + a_{\text{N}(5-\text{NO}_2)}$ is observed.

Table II. Experimental and Calculated hfs Constants (G) of 3,5-Dinitropyridine and 3-Nitropyridine Anion Radicals

Ring position	Nucleus	3,5-Dinitropyridine					3-Nitropyridine	
		Free anion			Ion pair		Ion pair	
		Exptl	Calcd		Exptl	Calcd	Exptl	Calcd
		<i>a</i>	<i>b</i>	<i>c</i>	<i>d</i>	<i>e</i>	<i>f</i>	<i>e</i>
1	N (-N=)	1.45	-2.03	2.97	1.37	2.09	1.21	1.43
3	N (NO ₂)	3.52	2.13	4.06	8.82	9.79	9.43	10.67
5	N (NO ₂)	3.52	2.13	4.06	0.27	0.49	1.03 ^g	1.29 ^g
2	H	4.85	-4.48	-7.06	3.53	-4.58	3.07	-3.11
6	H	4.85	-4.48	-7.06	5.11	-5.49	4.03	-4.20
4	H	3.36	-1.21	0.45	3.63	-2.19	3.42	-3.89
	Na				0.25		0.19	

^a Electrolytic reduction in THF. ^b INDO method.⁵ ^c Spin densities calculated by the McLachlan method¹⁷ and translated into coupling constants according to the relationships $a_{\text{H}} = -24.7\rho_{\text{C}} \text{ G}$,²⁴ $a_{\text{N}(\text{NO}_2)} = 33.0(2\rho_{\text{N}} - \rho_{\text{O}}) \text{ G}$,²⁴ $a_{\text{N}(-\text{N}=\text{O})} = 13.1\rho_{\text{N}} + 6.96(\rho_{\text{C}_2} + \rho_{\text{C}_6}) \text{ G}$.³⁹ ^d In THF. ^e Spin densities calculated by the McLachlan method¹⁷ modified according to McClelland.¹⁸ The cation is in the molecular plane at 1.5 Å from the nitrogen of the nitro group along the C-NO₂ bond. ^f In DME. ^g Proton at position 5.

DME and THF (Fluka) were carefully purified and the reaction with alkali metals was carried out according to the standard techniques.¹³ NaBPh₄ was progressively added through known volumes of titrated solution.

ESR spectra were recorded with a Varian E-Line Century Series spectrometer. The magnetic field sweep was calibrated by a Varian Field/Frequency Lock E-272B.

The temperatures were locked by a thermoresistance controlling a nitrogen flow through an electrovalve. The precision of temperature measurement was estimated to be 0.5 °C.

Methods of Calculations

The ab initio unrestricted Hartree-Fock wave function of the anionic component of the ion pair has been calculated by the GAUSSIAN 70 program¹⁴ adopting a STO-3G minimal basis set.¹⁵ The geometry of the radical anion was derived from that of the neutral molecule obtained by x-ray diffraction,¹⁶ assuming C_s symmetry with bond lengths and bond angles obtained by averaging the experimental values, except for the C-H bond length, for which the value 1.085 Å was assumed. The electrostatic interaction energy of the free anion with a unit point charge⁸ was calculated by using the ab initio uhf wave function of the radical anion; it was computed in the molecular plane and in parallel planes at 1.5, 2.0, 2.5, and 3.0 Å.

A different calculation was performed to include the influence of the cation on the spin distribution of the anion: we used the McLachlan method¹⁷ correcting the Hückel parameters for the electrostatic attraction between the anion radical and the cation, according to McClelland.¹⁸

DNP Anion/Alkali Metal Cation Ion Pairs. Experimental Results

The hfs constants of the system $\text{DNP}^-\cdot\text{M}^+$ were measured

in the range from -100 to 90 °C; no significant change was found on temperature variation. A typical spectrum is shown in Figure 1. In Table I we report the hfs constants for Li, Na, K, and Cs salts of $\text{DNP}^-\cdot$ in DME and THF at room temperature together with those of the radical anion obtained by electrolytic reduction in THF. In the case of the sodium salt the hfs constants obtained from spectra recorded at 20 and -60 °C after addition of NaBPh₄ are also reported. No results for Rb salts are included since their spectra are poorly resolved and their interpretation is complicated by the presence of the two Rb isotopes. Cs salts in DME are not soluble enough to record well-resolved spectra. Hfs patterns for Li, Na (before addition of NaBPh₄), K, and Cs salts are consistent with a spin distribution which does not have a C_s symmetry, unlike that of the free ion.⁷ In these spectra the 2,6 protons are not equivalent and the 1:2:3:2:1 hyperfine quintet of the two nitro groups is replaced by two 1:1:1 triplets with very different splittings of about 8.0 and 0.2 G, respectively. In the case of Li, Na, and Cs salts the quartets and the septet typical of these metals are easily recognized. These data suggest that the cation is localized near one nitro group to form a strongly associated ion pair. This classification is supported by the slight dependence of the hfs constants on temperature (Figure 2). Both the lack of valuable line-width alternation due to dynamic processes and the absence of the free ion spectrum in the whole range of temperatures confirm our interpretation.

Theoretical Model for the Ion pairs

The loss of symmetry in the spin distribution of the ion pair is well reproduced by the McLachlan method¹⁷ modified according to McClelland,¹⁸ the results are collected in Table II, together with the measured and calculated hfs constants of 3-nitropyridine⁻·Na⁺ ion pair in DME. The close correspon-

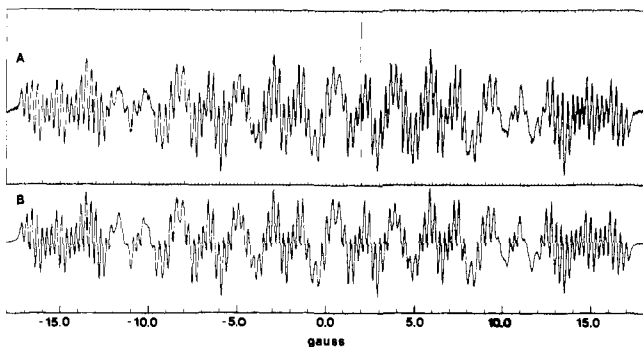


Figure 1. ESR spectra of $\text{DNP}^{\bullet-}\text{Na}^+$ in DME at 30 °C. (A) Experimental spectrum (modulation amplitude 0.16 G; microwave power 2 mW; time constant 0.25 s; scan rate 2.5 G/min). (B) Simulated spectrum: $a_{\text{N}(\text{NO}_2)} = 8.848 \pm 0.001$, $a_{\text{N}(\text{NO}_2)} = 0.269 \pm 0.002$, $a_{\text{N}(-\text{N}=\text{O})} = 1.373 \pm 0.001$, $a_{\text{H}_6} = 5.100 \pm 0.001$, $a_{\text{H}_4} = 3.634 \pm 0.001$, $a_{\text{H}_2} = 3.529 \pm 0.001$, $a_{\text{Na}} = 0.296 \pm 0.001$ G, and $W_0 = 0.153 \pm 0.002$ G.

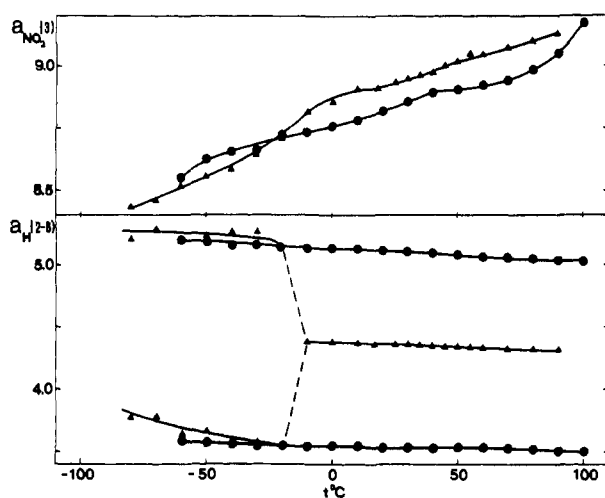


Figure 2. Temperature dependence of the hfs constants (G) of $\text{DNP}^{\bullet-}\text{Na}^+$ in DME (●) and DME containing 0.4 M NaBPh_4 (▲). The full lines were obtained through the trial interpolating function: $\log(aT) = a_0 + a_1(1/T) + a_2(1/T^2) + \dots = a_0(1 - a_1/a_0T)^{-1}$.

dence between the two experimental spin distributions and the comparison with the calculated values allow us to assign the larger proton splitting to the 6 proton (i.e., para to the nitro group near the cation) and the two nearly equivalent hfs constants to the 2,4 protons (i.e., ortho positions).

The calculated potential surfaces of $\text{DNP}^{\bullet-}$ in the molecular plane and in parallel planes at 1.5 and 3.0 Å are shown in Figures 3–5. By assuming that an alkali metal cation should not approach the anion closer than 1.5 Å, we discuss our results in term of envelope surfaces at distances between 1.5 and 3.0 Å from the anion. The absolute minimum of -130 kcal/mol is in the molecular plane in the region at 1.5 Å from the nitro group. A relative minimum (-115 kcal/mol) is found at the same distance in the region of ring nitrogen. There is no barrier between the oxygens of the same nitro group. Instead the barriers between the two nitro groups and between the nitro groups and the ring nitrogen are about 50 kcal/mol. These barriers sharply reduce to a few kilocalories per mole on the envelope at 3.0 Å from the anion. It emerges from Figure 5 that at 3.0 Å over the molecular plane the potential surface shows a flat minimum spread on the whole radical. These results confirm that the cation is localized in the region of one nitro group in agreement with spectroscopic evidence. The large values of the barrier between the two nitro groups prevent the intramolecular exchange of the cation and explain why line-

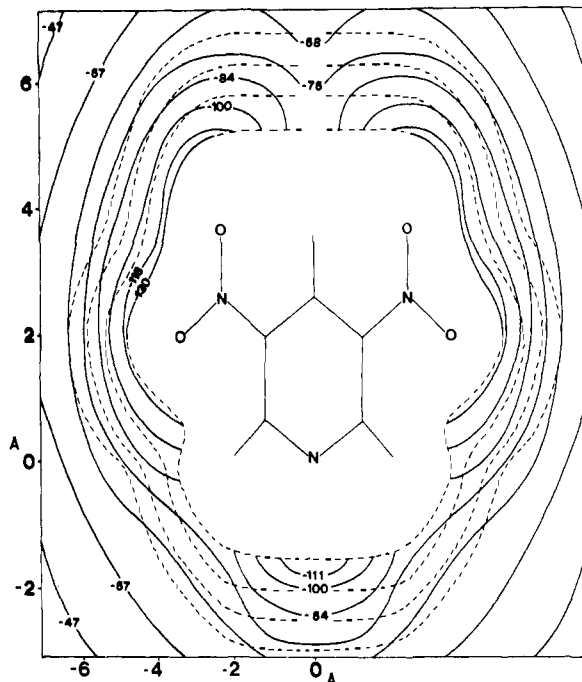


Figure 3. Contour lines of the electrostatic interaction energy between $\text{DNP}^{\bullet-}$ and a unit point charge: molecular plane. The lines connect isopotential points and the numbers represent the values in kcal/mol. The dotted lines represent the envelope surfaces at distances of 1.5, 2.0, 2.5, and 3.0 Å from the anion.

width alternation effects are not present in the ESR spectra of the ion pairs.

Sodium Exchange between Two Equivalent Sites

When small amounts of NaBPh_4 up to 0.4 M are added to a solution of $\text{DNP}^{\bullet-}\text{Na}^+$ the following significant changes occur in the ESR spectra: (a) the sodium quartet disappears and the large coupling constant of the nitro group nitrogen smoothly decreases; these facts, and in particular the decrease of the hfs constant with the addition of salt, are due to the formation of triple ions, which exist in rapid equilibrium with the ion pairs; (b) a very strong line-width alternation is observed in the hyperfine pattern; it can be evidenced by changing either the salt concentration or the temperature. The largest variations of line width on temperature are found for the doublets of 2 and 6 protons: above -30 °C in THF and -10 °C in DME the two doublets collapse into a triplet of about 4.3 G (Figure 2 and Table I), whose central line ($m_{\text{H}_2} + m_{\text{H}_6} = 0$) is broadened. This broadening decreases on increasing temperature, as shown in Figure 6. These line-width alternation effects are generated by a cation exchange between two equivalent positions at rates (see next sections and Table III) comparable to the difference between the two hfs constants ($|\Delta a| \approx 1.6|\gamma_e|s^{-1}$) expressed in frequency units.^{19–21} This condition is not fulfilled in the case of the two nitro groups ($|\Delta a| \approx 8.6|\gamma_e|s^{-1}$), so that the hyperfine lines with $M_N = \pm 1$ are completely broadened in the whole range of temperatures. The exchange frequency decreases with temperature and reaches the slow exchange limit at the lowest explored temperatures. The corresponding spectra consist of a superposition of individual spectra, whose time average is seen in the fast exchange region. In Table I the hfs constants determined at 20 (fast exchange region) and -60 °C (very slow exchange region) are shown.

The same exchange process was observed by Adams and Atherton¹¹ for the $\text{MDNB}^{\bullet-}\text{Na}^+$ ion pair in DME and THF containing NaBPh_4 . We reinvestigated these systems to get data processed by the same numerical method (see next sec-

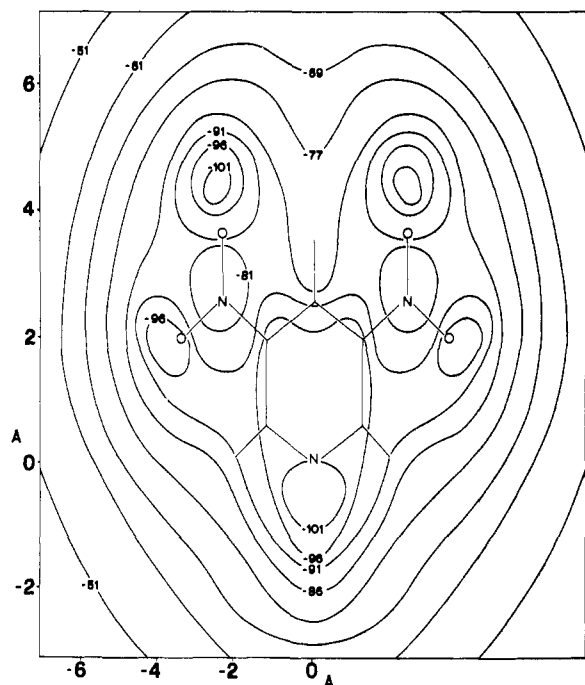


Figure 4. Contour lines of the electrostatic interaction energy between $\text{DNP}^{\bullet-}$ and a unit point charge: plane 1.5 Å over the molecular plane.

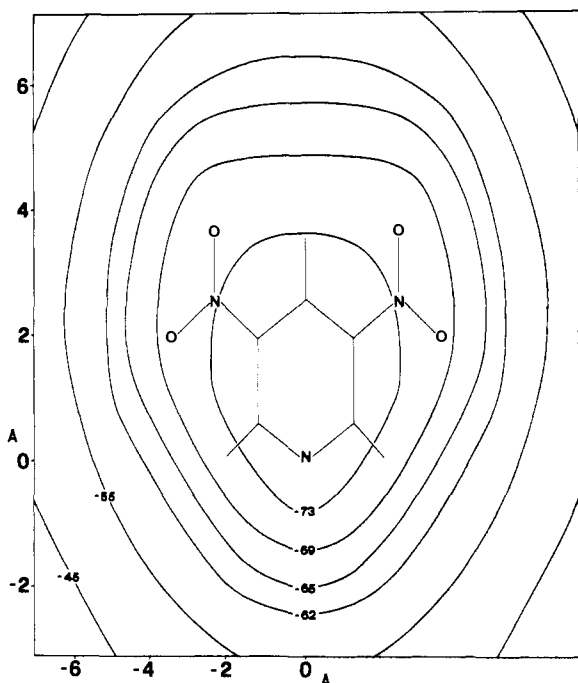


Figure 5. Contour lines of the electrostatic interaction energy between $\text{DNP}^{\bullet-}$ and a unit point charge: plane 3.0 Å over the molecular plane.

tion) and so comparable with those of the $\text{DNP}^{\bullet-}\cdot\text{Na}^+/\text{Na}^+\text{BPh}_4^-$ system.

ESR Line Shape Analysis

The effect of the chemical exchange process on line shape was calculated in a few cases by the general phenomenological density matrix method.^{22,23} The details of this application have been described elsewhere.²⁴ In most cases, to save computer time, we have adopted the formalism of the Redfield-Freed-Fraenkel theory¹⁹⁻²¹ valid in the fast exchange region. The following line-width expression was used:

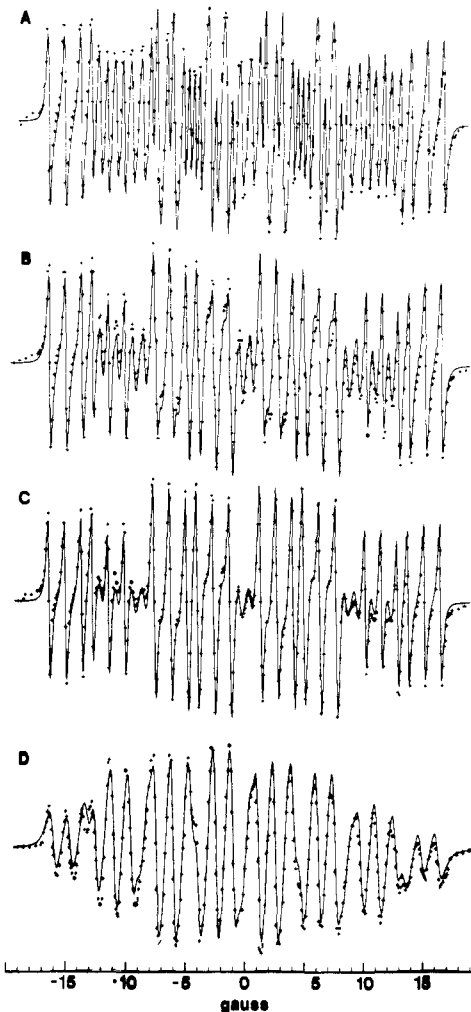


Figure 6. ESR spectra of $\text{DNP}^{\bullet-}\cdot\text{Na}^+$ in DME containing 0.4 M NaBPh_4 at different temperatures. Solid lines: simulated spectra; points: experimental spectra. (A) $t = 80^\circ\text{C}$; $a_{\text{N}(\text{NO}_2)} = 9.102 \pm 0.002$, $a_{\text{N}(-\text{N}=\text{N})} = 1.359 \pm 0.002$, $a_{\text{H}^{\text{triplet}}} = 4.321 \pm 0.002$, $a_{\text{H}^{\text{doublet}}} = 3.607 \pm 0.004$ G, and $W_0 = 0.273 \pm 0.006$, $W_{\text{exch}} = 0.136 \pm 0.006$ G, $\tau^{-1} = (2.48 \pm 0.15) \times 10^8 \text{ s}^{-1}$. (B) $t = 40^\circ\text{C}$; $a_{\text{N}(\text{NO}_2)} = 8.969 \pm 0.003$, $a_{\text{N}(-\text{N}=\text{N})} = 1.361 \pm 0.003$, $a_{\text{H}^{\text{triplet}}} = 4.349 \pm 0.002$, $a_{\text{H}^{\text{doublet}}} = 3.616 \pm 0.005$ G, and $W_0 = 0.296 \pm 0.008$, $W_{\text{exch}} = 0.258 \pm 0.009$ G, $\tau^{-1} = (1.31 \pm 0.07) \times 10^8 \text{ s}^{-1}$. (C) $t = 25^\circ\text{C}$; $a_{\text{N}(\text{NO}_2)} = 8.931 \pm 0.003$, $a_{\text{N}(-\text{N}=\text{N})} = 1.371 \pm 0.003$, $a_{\text{H}^{\text{triplet}}} = 4.370 \pm 0.002$, $a_{\text{H}^{\text{doublet}}} = 3.626 \pm 0.005$ G, and $W_0 = 0.259 \pm 0.008$, $W_{\text{exch}} = 0.374 \pm 0.022$ G, $\tau^{-1} = (0.90 \pm 0.07) \times 10^8 \text{ s}^{-1}$. (D) $t = -50^\circ\text{C}$ (very slow exchange region); $a_{\text{N}(\text{NO}_2)} = 8.568 \pm 0.011$, $a_{\text{N}(-\text{N}=\text{N})} = 1.416 \pm 0.009$, $a_{\text{H}_6} = 5.218 \pm 0.027$, $a_{\text{H}_2} = 3.532 \pm 0.036$, $a_{\text{H}_4} = 3.671 \pm 0.047$ G, and $A = 0.624 \pm 0.036$, $B_{\text{N}(\text{NO}_2)} = 0.030 \pm 0.010$, $C_{\text{N}(\text{NO}_2)} = 0.063 \pm 0.018$ G.

$$W(m_{\text{H}_2}, m_{\text{H}_6}) = W_0 + W_{\text{exch}}(m_{\text{H}_2} - m_{\text{H}_6})^2 = W_0 + W_{\text{exch}}(1 - M_{\text{H}}^2) \quad (1)$$

where $M_{\text{H}} = m_{\text{H}_2} + m_{\text{H}_6}$. W_0 is the width of a line not affected by the dynamic process and W_{exch} is the exchange contribution to the line width.

As the spectra, mainly at low temperatures, show also relaxation broadenings, such additional effects on line shape were taken into account through the well-known equation

$$W_j = A + \sum_{\alpha=1}^N B_{\alpha} \tilde{M}_{j\alpha} + \sum_{\alpha=1}^N C_{\alpha} \eta(M_{j\alpha}) + \sum_{\alpha < \beta} E_{\alpha\beta} \tilde{M}_{j\alpha} \tilde{M}_{j\beta} \quad (2)$$

(For a justification of eq 2 and related symbols see ref 20 and 21). The relevant spectral parameters were optimized through

Table III. Line-Width Contributions and Frequencies of the Intermolecular Cation Transfer for DNP⁻·Na⁺ and MDNB⁻·Na⁺ in DME and THF containing NaBPh₄^a

<i>t</i> , °C	DNP ⁻ ·Na ⁺ ^b		MDNB ⁻ ·Na ⁺ ^c	
	<i>W</i> _{exch} , G	$\tau^{-1} \times 10^{-7}$, s ⁻¹	<i>W</i> _{exch} , G	$\tau^{-1} \times 10^{-7}$, s ⁻¹
DME				
90	0.108 ± 0.007	3.13 ± 0.24		
80	0.136 ± 0.006	2.48 ± 0.15		<i>d</i>
70	0.165 ± 0.005	2.05 ± 0.11	0.018 ± 0.009	3.27 ± 1.64
60	0.185 ± 0.007	1.83 ± 0.11	0.022 ± 0.003	2.67 ± 0.37
55	0.194 ± 0.012	1.74 ± 0.13	0.016 ± 0.003	3.68 ± 0.69
50	0.199 ± 0.008	1.70 ± 0.10	0.027 ± 0.004	2.18 ± 0.33
45	0.219 ± 0.007	1.54 ± 0.08	0.024 ± 0.003	2.45 ± 0.31
40	0.258 ± 0.009	1.31 ± 0.07	0.025 ± 0.006	2.35 ± 0.57
35	0.317 ± 0.012	1.07 ± 0.06	0.035 ± 0.004	1.68 ± 0.19
30	0.361 ± 0.017	0.94 ± 0.06	0.045 ± 0.006	1.28 ± 0.17
25	0.374 ± 0.022	0.90 ± 0.07	0.055 ± 0.012	1.07 ± 0.23
20	0.458 ± 0.030	0.74 ± 0.06	0.067 ± 0.015	0.88 ± 0.19
10	0.544 ± 0.065	0.62 ± 0.08	0.073 ± 0.016	0.81 ± 0.18
0	0.858 ± 0.157	0.39 ± 0.07	0.104 ± 0.009	0.55 ± 0.05
-10	1.178 ± 0.355	0.29 ± 0.09	0.125 ± 0.010	0.47 ± 0.04
-20			0.154 ± 0.012	0.38 ± 0.03
-30			0.202 ± 0.014	0.29 ± 0.02
-40		<i>e</i>	0.270 ± 0.014	0.22 ± 0.01
-50			0.334 ± 0.020	0.18 ± 0.01
-60				<i>e</i>
THF				
90	0.058 ± 0.006	6.75 ± 0.71		
70	0.062 ± 0.007	6.32 ± 0.72		<i>d</i>
50	0.096 ± 0.008	4.08 ± 0.35		
40	0.114 ± 0.013	3.44 ± 0.40		
30	0.132 ± 0.015	2.97 ± 0.34	0.012 ± 0.007	6.68 ± 3.96
20	0.176 ± 0.014	2.23 ± 0.18	0.013 ± 0.006	6.16 ± 2.92
10	0.231 ± 0.014	1.70 ± 0.11	0.021 ± 0.010	3.82 ± 1.86
-10	0.437 ± 0.055	0.90 ± 0.11	0.033 ± 0.011	2.43 ± 0.85
-20	0.508 ± 0.059	0.77 ± 0.09	0.021 ± 0.014	3.82 ± 2.58
-30	1.062 ± 0.595	0.37 ± 0.21	0.044 ± 0.026	1.82 ± 1.09
-40			0.065 ± 0.022	1.23 ± 0.44
-50		<i>e</i>	0.082 ± 0.026	0.98 ± 0.33
-60			0.116 ± 0.033	0.69 ± 0.21
-70				<i>e</i>

^a 0.04 M for the DNP⁻·Na⁺/THF system; 0.4 M otherwise. ^b $|a_{H_2} - a_{H_6}| = 1.63$ G in DME and 1.76 G in THF, as obtained at the lowest explored temperatures (very slow exchange region). ^c $|a_{H_2} - a_{H_6}| = 0.68$ G in DME and 0.79 G in THF. ^d Very fast exchange region. ^e Very slow exchange region.

Table IV. Arrhenius Parameters of the Rates of the Line-Broadening Process

Ion pair	<i>E</i> _a kcal/mol ^a		10 ⁻¹⁰ <i>A</i> , s ⁻¹	
	THF	DME	THF	DME
DNP	4.21 ± 0.15	4.41 ± 0.14	9.1 ± 0.4 ^c	1.5 ± 0.3
MDNB ^b	3.69 ± 0.23	4.02 ± 0.21	4.0 ± 0.8	1.2 ± 0.4

^a Half a value of the dissociation heat of NaBPh₄ has to be subtracted in order to obtain the activation energy of the rate constant *k*_f ($\Delta H_D = -1.3$ and -1.7 kcal/mol in THF and DME, respectively).²⁶ ^b The values previously reported (*E*_a = 6.2 kcal/mol, *A* = 1.3 × 10¹² s⁻¹)¹¹ are probably affected by the narrow range of explored temperatures. ^c Corrected for a 0.4 M concentration of NaBPh₄.

an iterative least-squares line shape fitting procedure. A modified version of the computer program ESRCON,²⁵ reproducing the exchange and the relaxation effects on line shape and optimizing parameters *W*_{exch}, *A*, *B*_α, *C*_α, and *E*_{αβ}, was used.²⁴

Calculation of Sodium Exchange Frequency

The frequency τ^{-1} of the cation transfer is related to the exchange contribution to the line width, *W*_{exch}, through the following relationship:^{20,21}

$$\tau^{-1} (\text{s}^{-1}) = \frac{|\gamma_e|}{8\sqrt{3}} \cdot \frac{|a_{H_2} - a_{H_6}|^2}{W_{\text{exch}}} \quad (3)$$

where $|\gamma_e|/8\sqrt{3} = 1.271 \times 10^6$ G⁻¹ s⁻¹ if *a*_H and *W*_{exch} are

expressed in gauss. The value of $|a_{H_2} - a_{H_6}|$ was assumed to be temperature independent and was evaluated from the corresponding ESR spectra in the very slow exchange region. Exchange frequencies and line-width coefficients are collected in Table III. By matching the calculated with the experimental rate constants over the explored range of temperatures, we have determined the activation parameters for the dynamic process involved. The corresponding Arrhenius plots are given in Figure 7. The Arrhenius parameters derived therefrom are collected in Table IV.

Mechanism of Cation Exchange

The exchange contribution (*W*_{exch}) to the line width was found to depend on the concentration of added NaBPh₄, as

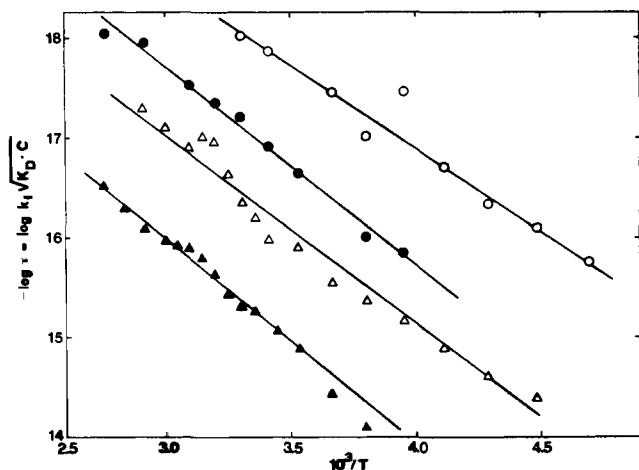


Figure 7. Arrhenius plots of the rates of the line-broadening process. (O) MDNB⁻·Na⁺/THF/Na⁺BPh₄⁻; (●) DNP⁻·Na⁺/THF/Na⁺BPh₄⁻; (Δ) MDNB⁻·Na⁺/DME/Na⁺BPh₄⁻; (▲) DNP⁻·Na⁺/DME/Na⁺BPh₄⁻ (scale shifted by -0.75).

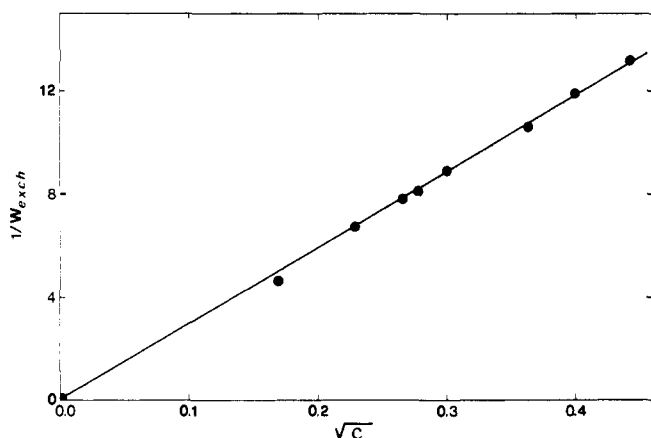
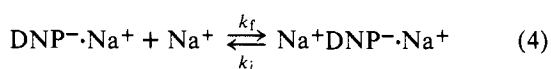


Figure 8. Plot of $1/W_{\text{exch}}$ vs. the square root of the NaBPh₄ concentration (M) for the DNP system in THF.

shown in Figure 8. The observed salt dependence of W_{exch} as well as that of the nitrogen splitting of the nitro groups can be attributed to the reaction



The rate of the line-broadening process is first order in sodium ion concentration, according to the plot of Figure 8 and the following relation:

$$\tau^{-1} = \frac{1}{[\text{DNP}^{\cdot-}\text{Na}^+]} \cdot \frac{d[\text{DNP}^{\cdot-}\text{Na}^+]}{dt} = k_f[\text{Na}^+] \approx k_f\sqrt{K_D C} \quad (5)$$

where the mean lifetime (τ) between cation exchanges is given by eq 3; C is the molar concentration of added NaBPh₄ and K_D is its dissociation constant.²⁶ The rate was independent of the concentrations of DNP and of the ion pair. From the plot of Figure 8 a value of $k_f = (122.8 \pm 0.6) \times 10^8 \text{ M}^{-1} \text{ s}^{-1}$ was determined at 20 °C.

The presence of triple ion in dilute ethereal solutions of radical ions having two polar groups in symmetric positions has been reported on several occasions.²⁷⁻³² The structures of such species^{23,30-32} and the possible roles of these species in intermolecular cation-transfer reactions^{11,29,32-34} have been discussed recently. In our case the presence of the triple ion in solution with the ion pair leads to an ESR spectrum due to a

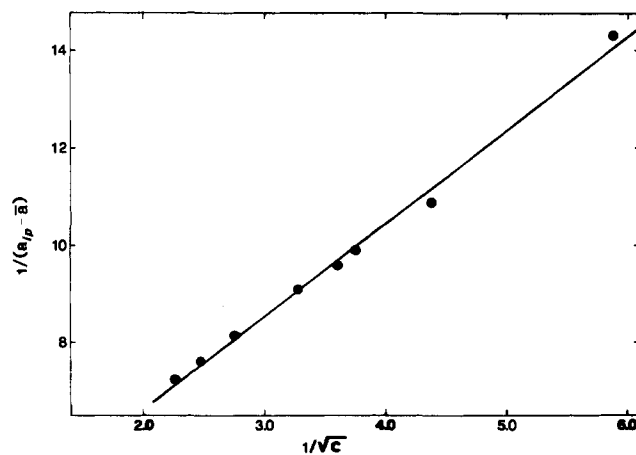


Figure 9. Plot of $1/(a_{\text{ip}} - \bar{a})$ vs. the reciprocal of the square root of the NaBPh₄ concentration (M) for the DNP system in THF.

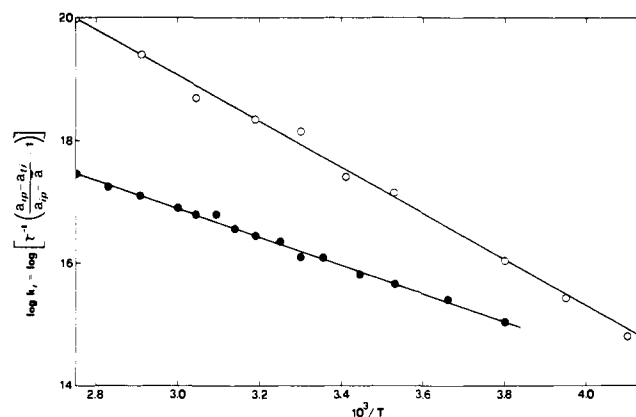


Figure 10. Arrhenius plots of the rate constants of the Na⁺DNP⁻·Na⁺ triple ion ionization in THF (O) and DME (●).

time-averaged species: the observed hfs coupling constants are the results of the time average (\bar{a}) between the coupling constants of the triple ion (a_{ti}) and the ion pair (a_{ip}). According to the procedure given by Stevenson and co-workers,³⁵ the following relationship is obtained:

$$\frac{1}{a_{\text{ip}} - \bar{a}} = \frac{1}{a_{\text{ip}} - a_{\text{ti}}} + \frac{1}{(a_{\text{ip}} - a_{\text{ti}})K_T\sqrt{K_D C}} \quad (6)$$

where $K_T = k_f/k_i$ is the thermodynamic equilibrium constant controlling the formation of the triple ion. Provided that a plot of $1/(a_{\text{ip}} - \bar{a})$ vs. $1/\sqrt{C}$ is linear, K_T can be obtained from the slope and the intercept. Treated in this manner, our data did yield a straight line, as shown in Figure 9, with an equilibrium constant of $156 \pm 13 \text{ M}^{-1}$ at 20 °C. A value of $4.366 \pm 0.003 \text{ G}$ was obtained for the nitrogen hfs constant of the two nitro groups in the triple ion. By combining eq 5 and 6 the rate constant k_i is readily obtained:

$$k_i = \tau^{-1} \left(\frac{a_{\text{ip}} - a_{\text{ti}}}{a_{\text{ip}} - \bar{a}} - 1 \right) \quad (7)$$

The corresponding Arrhenius plots are shown in Figure 10. The dependence of τ , a_{ip} , and \bar{a} on temperature was known from the experiments, whereas the difference ($a_{\text{ip}} - a_{\text{ti}}$) was kept constant. The following activation parameters for the ionization of Na⁺DNP⁻·Na⁺ were derived:

DME

$$E_a = 4.60 \pm 0.08 \text{ kcal/mol}, A = (2.3 \pm 0.3) \times 10^{10} \text{ s}^{-1}$$

THF

$$E_a = 7.56 \pm 0.14 \text{ kcal/mol}, A = (1.8 \pm 0.4) \times 10^{13} \text{ s}^{-1}$$

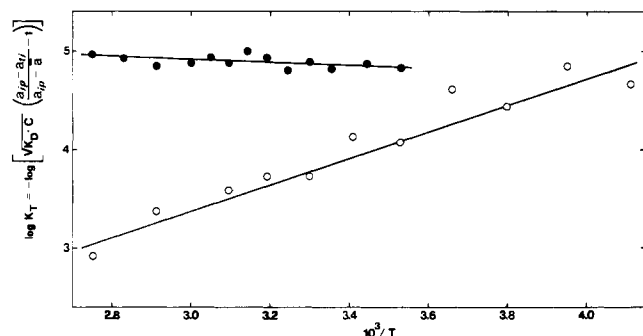


Figure 11. Plots of $\log K_T$ vs. $1/T$ for the DNP system in THF (O) and DME (●).

The values of K_T at each of the temperatures studied can be easily obtained by eq 6. These data were treated in the usual manner (Figure 11) to yield the values -2.58 ± 0.21 kcal/mol and ~ 0 eu for the enthalpy and entropy in the THF, respectively. In DME the equilibrium constant did not change significantly in the whole range of temperatures ($K_T = 211 \text{ M}^{-1}$; $\Delta H \approx 0$ kcal/mol, $\Delta S = 11.5 \pm 0.4$ eu). The major deviations in the plots of Figures 7 and 11 should be ascribed to the difficulty in obtaining accurate values of K_D at each temperature. Moreover, the plot of $\log K_D$ vs. $1/T$ is not linear in the whole range of temperatures.²⁶

The ascertained dependence of the observed rate of the line-broadening process on salt concentration and the formation of triple ions indicate that the cation transfer in the $\text{DNP}^- \cdot \text{Na}^+$ ion pair is intermolecular. The two mechanisms firstly suggested by Adams and Atherton¹¹ for $\text{MDNB}^- \cdot \text{Na}^+$ can be formulated also for $\text{DNP}^- \cdot \text{Na}^+$ (see Figure 12A,B). These mechanisms produce different line-width effects. In the case of (A) the hyperfine components of 2,6 protons triplets broaden according to the relationship^{20,21} $W(M_H) = W_O + W_{\text{exch}} M_H^2$, whereas in (B) eq 1 holds. Our observations are consistent with mechanism (B).

A Simple Theoretical Model for the Reaction Path of the Intermolecular Cation Transfer in the Systems $\text{DNP}^- \cdot \text{Na}^+ / \text{Na}^+ \text{BPh}_4^-$ and $\text{MDNB}^- \cdot \text{Na}^+ / \text{Na}^+ \text{BPh}_4^-$

The association energy of $\text{DNP}^- \cdot$ with two point charges has been calculated according to the McClelland method.¹⁸ By defining r_1 and r_2 as shown in Figure 12B, and assuming $r_1 + r_2 = \text{const}$, r_1 was chosen as the reaction coordinate in the cation exchange between $\text{DNP}^- \cdot \text{Na}^+$ and $\text{Na}^+ \text{BPh}_4^-$ ion pairs. The cations have been allowed to move along the directions of the C-NO₂ bonds in the molecule plane as far as 18 Å. Beyond this distance the cation does not perturb the spin distribution of the ion pair. The trend of the association energy vs. r_1 is plotted in Figure 12B. A similar trend has been obtained for $\text{MDNB}^- \cdot \text{Na}^+$. The barrier height is lower for $\text{MDNB}^- \cdot \text{Na}^+$ than for $\text{DNP}^- \cdot \text{Na}^+$; the difference of about 0.4 kcal/mol between the two barriers reproduces well the experimental difference of the activation energies (see Table IV) for intermolecular cation transfer.

Effect of Solvent Viscosity

To obtain information about the effect of solvent viscosity on the kinetics of the cation exchange, we have evaluated the activation energy of the diffusion process. According to the rotational diffusion model for the electron spin relaxation in liquids,³⁶ the coefficients B_α and C_α of eq 2 are proportional to η/T . As the solvent viscosity η follows a Boltzmann distribution,²⁶ the plots of $\log(B_\alpha T)$ or $\log(C_\alpha T)$ vs. $1/T$ lead to

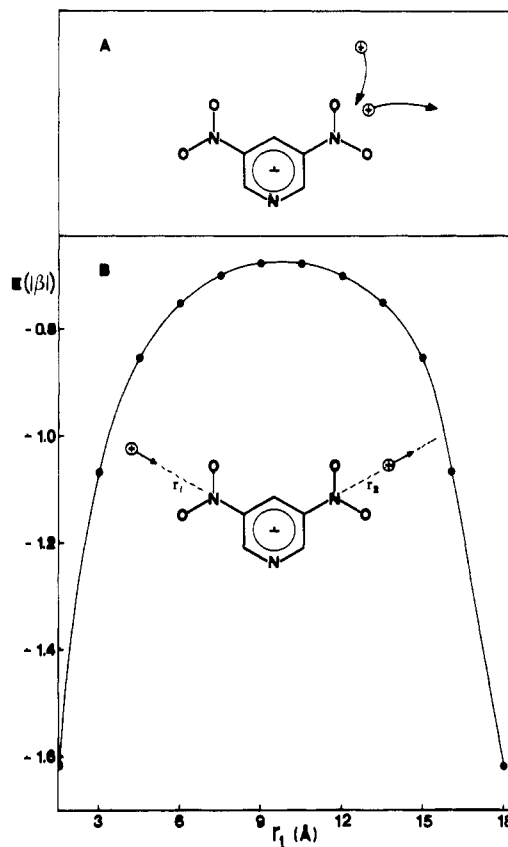


Figure 12. Possible reaction mechanisms of sodium cation exchange in the DNP system (see text). The energy barrier calculated through the McClelland method is reported for mechanism (B).

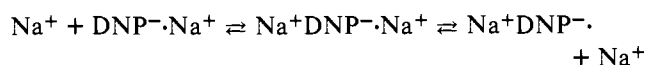
the following activation energies:

$$\begin{aligned} \text{DME} + \text{NaBPh}_4 (0.4 \text{ M}) & \quad -E_\eta = 2.58 \pm 0.09 \text{ kcal/mol} \\ \text{THF} + \text{NaBPh}_4 (0.4 \text{ M}) & \quad -E_\eta = 2.29 \pm 0.34 \text{ kcal/mol} \\ & \quad \Delta E_\eta = 0.29 \text{ kcal/mol} \end{aligned}$$

As these values are less than the activation energies for the intermolecular cation transfer (see Table IV), it can be inferred that the diffusion is not the rate-determining step. However, the difference ΔE_η of about 0.3 kcal/mol may account for the difference between the activation energies of chemical exchange in DME and THF.

Concluding Remarks and Summary

When DNP reacts in ethereal solvents with the alkali metals, the corresponding ion pairs are formed. The ESR spectra show that the cation is strongly associated to the anion in the region of the nitro group. The finding is supported by the analysis of the potential surface of the radical anion computed by using an ab initio wave function. The calculated barrier of about 50 kcal/mol between the two nitro groups prevents the intramolecular transfer of the alkali metal cation between the two regions of highest electron density. The fact accords well with the observation that the shapes of ESR lines are unaffected by cation transfer. However, through the line shape analysis of the ESR spectra after the addition of NaBPh_4 to the ion pair solution, the following reaction mechanism can be established:



The intermolecular cation transfer via the formation of a symmetric triple ion is evidenced both by the line-width al-

ternation and the dependence of the nitrogen hfs constant on NaBPh_4 concentration. The kinetic parameters for the formation ($k_f = 122.8 \times 10^8 \text{ M}^{-1} \text{ s}^{-1}$ at 20°C in THF, $E_a = 4.9$ kcal/mol) and the ionization ($k_i = 7.7 \times 10^7 \text{ s}^{-1}$ at 20°C in THF, $E_a = 7.6$ kcal/mol) of the triple ion have been determined. The thermodynamic equilibrium constant controlling the formation of the triple ion in THF is 156 M^{-1} at 20°C ($\Delta H = -2.6$ kcal/mol, $\Delta S \approx 0$ eu). If $\text{DNP}^- \cdot \text{Na}^+$ forms a contact triple ion, one fully solvated Na^+ ion changes into a nonsolvated one, according to eq 4. Desolvation of ions increases the entropy of the system and makes the association endothermic.³⁷ As the heats of formation of the triple ion both in THF and in DME are low (-2.6 to 0 kcal/mol), it can be inferred that the triple ions as well as the ion pairs³⁸ are solvent separated.

References and Notes

- (1) Institute of Physical Chemistry, University of Sassari, 07100 Sassari, Italy.
- (2) M. Szwarc, "Ions and Ion Pairs in Organic Reactions", Vol. I and II, Wiley-Interscience, New York, N.Y., 1972, and references cited therein.
- (3) P. Cremaschi, A. Gamba, G. Morosi, C. Oliva, and M. Simonetta, *J. Chem. Soc., Faraday Trans. 2*, **71**, 189 (1975).
- (4) A. Gamba, C. Oliva, and M. Simonetta, *Chem. Phys. Lett.*, **36**, 88 (1975).
- (5) P. Cremaschi, A. Gamba, G. Morosi, C. Oliva, and M. Simonetta, *Gazz. Chim. Ital.*, **106**, 337 (1976).
- (6) P. T. Cottrell and P. M. Rieger, *Mol. Phys.*, **12**, 149 (1967).
- (7) A. Gamba, G. Morosi, C. Oliva, and M. Simonetta, *Gazz. Chim. Ital.*, **105**, 509 (1975).
- (8) E. Scrocco and J. Tomasi, *Top. Curr. Chem.*, **42**, 1 (1973).
- (9) P. Cremaschi, A. Gamba, and M. Simonetta, *Theor. Chim. Acta*, **40**, 303 (1975).
- (10) P. Cremaschi, A. Gamba, G. Morosi, and M. Simonetta, *Theor. Chim. Acta*, **41**, 177 (1976).
- (11) R. F. Adams and N. M. Atherton, *Trans. Faraday Soc.*, **64**, 7 (1968).
- (12) E. Plazek, *Recl. Trav. Chim. Pays-Bas*, **72**, 569 (1953).
- (13) M. Bonardi, Thesis, University of Milan, 1977.
- (14) W. J. Hehre, W. A. Lathan, R. Ditchfield, M. D. Newton, and J. A. Pople, GAUSSIAN 70, QCPE No. 236, Indiana University, Bloomington, Ind.
- (15) W. J. Hehre, R. F. Stewart, and J. A. Pople, *J. Chem. Phys.*, **51**, 2657 (1969).
- (16) R. Destro, T. Pilati, and M. Simonetta, *Acta Crystallogr., Sect. B*, **30**, 2071 (1974).
- (17) A. D. McLachlan, *Mol. Phys.*, **3**, 244 (1966).
- (18) B. J. McClelland, *Trans. Faraday Soc.*, **5A**, 1458 (1961).
- (19) A. G. Redfield, *IBM J. Res. Dev.*, **1**, 19 (1957); *Adv. Magn. Reson.*, **1**, 1 (1965).
- (20) J. H. Freed and G. K. Fraenkel, *J. Chem. Phys.*, **39**, 326 (1963).
- (21) G. K. Fraenkel, *J. Phys. Chem.*, **71**, 139 (1967).
- (22) J. I. Kaplan, *J. Chem. Phys.*, **28**, 278 (1958); **29**, 462 (1958).
- (23) S. Alexander, *J. Chem. Phys.*, **37**, 967, 974 (1962); **38**, 1787 (1963); **40**, 2741 (1964).
- (24) M. Barzaghi, P. L. Beltrame, G. Gamba, and M. Simonetta, *J. Am. Chem. Soc.*, **100**, 251 (1978).
- (25) J. Heinzer, ESRCON, QCPE, No. 197, Indiana University, Bloomington, Ind.
- (26) C. Carvajal, K. J. Tölle, J. Smid, and M. Szwarc, *J. Am. Chem. Soc.*, **87**, 5548 (1965).
- (27) J. V. Acrivos, *J. Chem. Phys.*, **47**, 5389 (1967).
- (28) T. E. Gough and P. R. Hindle, *Can. J. Chem.*, **47**, 1968, 3393 (1969).
- (29) A. W. Rutter and E. Warhurst, *Trans. Faraday Soc.*, **66**, 1866 (1970).
- (30) T. E. Gough and P. R. Hindle, *Trans. Faraday Soc.*, **66**, 2420 (1970).
- (31) S. A. Al-Baldawi and T. E. Gough, *Can. J. Chem.*, **48**, 2798 (1970); **49**, 2059 (1971).
- (32) K. S. Chen and N. Hirota, *J. Am. Chem. Soc.*, **94**, 5550 (1972).
- (33) A. W. Rutter and E. Warhurst, *Trans. Faraday Soc.*, **64**, 2338 (1968).
- (34) T. E. Gough and P. R. Hindle, *Can. J. Chem.*, **48**, 3959 (1970).
- (35) A. E. Alegria, R. Concepción, and G. R. Stevenson, *J. Phys. Chem.*, **79**, 361 (1975).
- (36) L. T. Muus and P. W. Atkins, "Electron Spin Relaxation in Liquids", Plenum Press, New York, N.Y., 1972.
- (37) (a) R. C. Roberts and M. Szwarc, *J. Am. Chem. Soc.*, **87**, 5542 (1965). (b) A reasonable value for the heat of solvation of Na^+ in DME is -7 kcal/mol [T. Shimmomura, J. Smid, and M. Szwarc, *J. Am. Chem. Soc.*, **89**, 5743 (1967)].
- (38) If we assume that there are rapid equilibria between contact and solvent-separated ion pairs in the $\text{DNP}^- \cdot \text{Na}^+$ system, the equilibrium constants can be evaluated from temperature dependence of the alkali metal splitting, according to the procedure given by Hirota [N. Hirota, *J. Phys. Chem.*, **71**, 127 (1967)]. Then the dissociation heat (-1.7 kcal/mol) and the change in the entropy of the system (-6 eu) can be evaluated in the usual manner. As only the time-averaged alkali metal splittings are known from the experiments, whereas the splittings for the contact and solvent-separated ion pairs can be only guessed, the uncertainties on the enthalpy and entropy values are about 50%. However the value of -1.7 kcal/mol, if compared with the dissociation heat of NaBPh_4 in ethereal solvents,²⁶ suggests that $\text{DNP}^- \cdot \text{Na}^+$ is a solvent-separated ion pair.
- (39) A. Gamba, V. Malatesta, G. Morosi, C. Oliva, and M. Simonetta, *J. Phys. Chem.*, **77**, 2744 (1973).

Nucleophilic Solvent Assistance in the Solvolysis of *endo*-2-Norbornyl Derivatives

J. Milton Harris,*^{1a} Dwight L. Mount,^{1a} and Douglas J. Raber*^{1b}

Contribution from the Department of Chemistry, The University of Alabama in Huntsville, Huntsville, Alabama 35807, and the Department of Chemistry, The University of South Florida, Tampa, Florida 33620. Received May 9, 1977

Abstract: *endo*-2-Norbornyl derivatives have in many instances served as models with which to compare the solvolysis of *exo*-2-norbornyl derivatives. Consequently, it is important that the solvolysis of the *endo* epimer be well characterized if the nature of *exo*-norbornyl solvolysis is to be determined. In the present paper nine probes of nucleophilic solvent assistance are applied to *endo*-norbornyl solvolysis, and it is determined that the amount of solvent assistance is small. The implications of this conclusion are considered.

That *endo*-2-norbornyl derivatives solvolyze with nucleophilic solvent assistance has become an important argument^{2,3} in the controversy⁴ over the nature of the 2-norbornyl cation. Winstein originally proposed⁶ that *endo*-2-norbornyl brosylate ionization is aided by weak nucleophilic solvent assistance to yield what is best described as a nucleophilically solvated ion pair, **1**, which then reacts further by collapsing (without rearrangement) to inverted solvolysis product, or undergoes leakage to the 2-norbornyl cation (Scheme I). Important supporting evidence for this conclusion was the observation of

8% excess inverted (unrearranged) acetate upon acetyloysis.^{6,7}

The work of Schleyer's group in the late 1960s established the importance of nucleophilic solvent assistance in the solvolysis of secondary derivatives,⁵ and this raised the possibility that such assistance might be important in the solvolysis of *endo*-2-norbornyl derivatives. While Schleyer himself has argued^{4a} that *endo*-2-norbornyl derivatives solvolyze with only weak solvent assistance, much greater importance has at times been suggested for the role of solvent in these reactions.^{2,3} The